The p47^{phox} Mouse Knock-Out Model of Chronic Granulomatous Disease

By Sharon H. Jackson, John I. Gallin, and Steven M. Holland

From the Laboratory of Host Defenses, National Institute of Allergy and Infectious Diseases, National Institutes of Health, Bethesda, Maryland 20892-1886

Summary

Chronic granulomatous disease (CGD) is caused by a congenital defect in phagocyte reduced nicotinamide dinucleotide phosphate (NADPH) oxidase production of superoxide and related species. It is characterized by recurrent life-threatening bacterial and fungal infections and tissue granuloma formation. We have created a mouse model of CGD by targeted disruption of p47^{phox}, one of the genes in which mutations cause human CGD. Identical to the case in human CGD, leukocytes from p47$^{phox-/-}$ mice produced no superoxide and killed staphylococci ineffectively. p47$^{phox-/-}$ mice developed lethal infections and granulomatous inflammation similar to those encountered in human CGD patients. This model mirrors human CGD and confirms a critical role for the phagocyte NADPH oxidase in mammalian host defense.

Phagocytes play a primary and essential role in host defense against microbes, in large part through the production of superoxide by the activation of a latent multicomponent phagocyte reduced nicotinamide dinucleotide phosphate (NADPH)[1] oxidase. The critical role of NADPH oxidase and its products of oxidative metabolism such as hydroxyl radical, superoxide, hydrogen peroxide, and hypochlorous acid (bleach) in host defense is demonstrated in humans by chronic granulomatous disease (CGD). CGD is a rare genetic childhood disease in which phagocytes do not produce these products, leading to severe infections with bacteria and fungi and early death (1-4). In addition to infections, CGD patients display aberrant inflammatory responses and tissue granuloma formation, the mechanism of which is not known (5-7). Beyond its role in host defense, a role for products of the NADPH oxidase in the generation of cataracts, malignant transformation, adult respiratory distress syndrome, and atherogenesis has been hypothesized (8, 9). Recently, IFN-γ, a proinflammatory cytokine, has been shown to be effective prophylaxis for the infectious complications of CGD (10).

Activation of the phagocyte NADPH oxidase requires the coordinated assembly of four structural proteins: the membrane-bound flavocytochrome$_{b558}$, composed of a heavy chain (gp91^{phox}, 11) and a light chain (p22^{phox}, 12), and three cytosolic proteins, p47^{phox} (13, 14), p67^{phox} (15), and the GTP-binding regulatory protein *rac* (16, 17). The X-linked form of CGD is caused by mutations in gp91^{phox} (60% of cases), while the autosomal recessive forms are caused by mutations

in p47^{phox} (30% of cases), p67^{phox} (5% of cases), and p22^{phox} (5% of cases) (18-21). The discovery of nitric oxide and the mouse macrophage nitric oxide synthase have disclosed novel mechanisms of intracellular killing (22, 23). The necessity of superoxide and related species for host defense in mammals that possess a phagocyte nitric oxide synthase is unknown.

Having previously shown that mouse p47^{phox} could functionally replace human p47^{phox} in a cell-free assay of superoxide production (24), we disrupted the mouse p47^{phox} gene to create a mouse model of CGD (25). p47$^{phox-/-}$ mice showed a condition identical to human CGD. Their phagocytes showed no respiratory burst activity and killed staphylococci poorly. At sites of infection, they developed granulomata. By 14 wk of age, 50% of animals developed spontaneous infections.

Materials and Methods

Generation of the Polyadenylated Neomycin Resistance Cassette. The neomycin resistance cassette was prepared by PCR as follows: EcoRV and SmaI recognition sites were generated flanking the 5' SV$_{40E}$/TK promoter site and the 3' PstI site of the polyadenylated neomycin resistance gene (pMC1neo poly A; Stratagene, La Jolla, CA). 5' primer 5'-ACGATATCCCCGGGCAGTGTGGTTTTGCAAGAG; 3' primer 5'-GAGATATCCCCGGGCTGCAGGTCGACGGATCC. The fragment was cloned into pBluescript (Stratagene) and transfected into NIH 3T3 cells, where it conveyed resistance to Geneticin (G418; GIBCO BRL, Gaithersburg, MD) at 500 μg/ml

Generation of the Homologous Recombination Construct. A 6-8 wk female B6/CBA mouse genomic DNA library in lambda FIX II (Stratagene) was screened with a 1.05-kb fragment, spanning nucleotides 18-1067 of the open reading frame, of mouse p47^{phox} cDNA as a probe (24). A 4.5-kb XbaI fragment containing exons 3-7 of p47^{phox} was subcloned into the pBluescript II(+/−) plasmid

---

[1] *Abbreviations used in this paper:* CGD, chronic granulomatous disease; ES, embryonic stem (cells); NADPH, reduced nicotinamide dinucleotide phosphate; NBT, nitroblue tetrazolium.

(Stratagene) and mapped. The replacement homologous recombination targeting construct was prepared by subcloning a 3.2-kb XbaI-PstI fragment from the 4.5-kb XbaI fragment into a BamHI-deleted pBluescript II(+/−) plasmid. The cloned XbaI-PstI fragment was cleaved at the contiguous BamHI sites in the 3′ terminus of exon 7. The sticky ends were blunted using Klenow, and the 1.15-kb neomycin resistance cassette was ligated into this site in the forward orientation. The elimination of both wild-type BamHI sites was confirmed by sequencing.

Generation of Homologous Recombinant Cell Lines. The embryonic stem cell line D3 (26) was kindly provided by Dr. Tak Mak (The Ontario Cancer Center, Princess Margaret Hospital; Toronto, Canada). Embryonic stem (ES) cells were cultured on mitomycin-C (10 μg/ml; Boehringer Mannheim Biochemicals, Indianapolis, IN)–treated primary embryonic fibroblasts derived from 15-d-old C57BL/6 embryos. Aliquots of 5 × 10^6 ES cells were electroporated with 20 μg of the linearized targeting construct. After electroporation, cells were immediately cultured with 10^3 U/ml murine leukemia inhibitory factor (ESGRO; Gibco BRL). 300 μg/ml geneticin was added 48 h after electroporation. Individual G418-resistant colonies were transferred to 96-well plates at ∼14 d for screening. G418-resistant colonies were screened by sib analysis PCR (27). PCR was performed in a 50-μl reaction containing 200 μM dNTP, 10 mM Tris-HCl, pH 8.3, 1.5 mM MgCl$_2$, 0.5 μM of each primer and 2 U *Taq* polymerase (Boehringer Mannheim). Cycling parameters were 96°C for 30 s, 60°C for 30 s, 72°C for 2 min for 35 cycles. The upstream primer 5′-ACGAGTTCTTCTGAG-GGGATCGGCAAT-3′ was located 63 bp internal to the 3′ terminus of the polyadenylated neomycin resistance cassette. The downstream primer 5′-CGTACGCCTTGATGGTTACATACG-3′ was located in the 5′ end of exon 8. Amplification of the 1.9-kb target band was confirmed by Southern analysis using a 1.8-kb internal probe. PCR-positive clones were further screened by Southern analysis with full-length mouse p47^{phox} cDNA and neo^r probes.

Generation of Homologous Recombinant Mice. Microinjection of two homologous recombinant ES cell clones, implantation of blastocysts into pseudopregnant females, and initial breeding of chimeric males were performed in the Transgenic Services Laboratories at The Rockefeller University (New York) according to standard techniques (28). Two fertile chimeric males were obtained from one homologous recombinant ES cell clone, IC5. Chimeric males were bred to C57BL/6J females. Agouti offspring heterozygous for the targeted disruption were identified by Southern analysis of XbaI- and BamHI-digested tail biopsy DNA probed with the p47^{phox} cDNA and neo^r fragments. p47^{phox} $^{+/-}$ animals were bred to each other to obtain homozygous homologous recombinants. The genotypes $^{+/+}$, $^{+/-}$, and $^{-/-}$ were determined by Southern analysis of Bam HI-digested tail biopsy DNA probed with the mouse p47^{phox} cDNA and neo^r fragments. Before entry into our animal facility, all animals tested negative for specific murine pathogens and were maintained in a specific pathogen-free environment. Animals were maintained in sterilized microisolator cages on autoclaved food, water, and bedding, and they were transferred to fresh cages weekly. Animal handling was performed by gloved handlers in an HEPA-filtered laminar flow hood. Gloves and hood surfaces were cleaned with the sterilant chlorine dioxide before animal handling. All necropsies were examined for sites of inflammation or infection, and all suspicious sites were cultured.

Determination of Biochemical Phenotype. For performance of the nitroblue tetrazolium test (NBT) (29–32), murine leukocytes in whole blood were adhered to a glass slide and then stimulated for 30 min at 37°C with 100 μl of equal parts 0.5 μg/ml PMA (Sigma Immunochemicals, St. Louis, MO) and 0.2% NBT (Sigma). Erythrocytes were washed off and leukocytes were counterstained with safranin. Flow cytometric analysis for respiratory burst activity was performed on PMA-stimulated whole blood as described (33).

In Vitro Staphylococcal Killing. 500 μl of blood was collected by tail venisection into microcentrifuge tubes containing 10 U
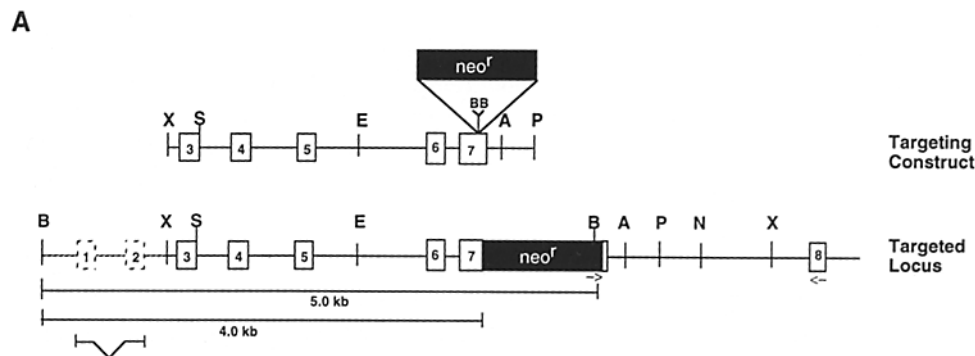

Figure 1. Targeted disruption of the p47^{phox} gene locus. (*A*) Design of the mouse p47^{phox} targeting construct. A 3.5-kb XbaI-PstI fragment of the mouse p47^{phox} gene containing exons 3–7 was subcloned and the 1.15-kb neomycin resistance (neo^r) cassette was cloned in the sense direction into the blunted BamHI sites in the 3′ terminus of exon 7. The positions of the primers used for PCR detection of recombinant ES cell clones are designated with arrows. The confirmatory probe for the PCR was a 1.8-kb fragment internal to the primers. The probe composed of exons 1 and 2 is indicated. Numbered solid outlined boxes represent mapped exons of p47^{phox}. Exons 1 and 2 (hatched line and boxes) have been mapped within the BamHI fragment but their exact location has not been determined. *A*, Asp718; *B*, BamHI; *E*, EcoRI; *P*, PstI; *N*, NcoI; *S*, SmaI; *X*, XbaI. (*B*) Southern analysis of BamHI-digested tail DNA from products of heterozygous matings using mouse p47^{phox} cDNA. The hybridizing BamHI fragment was augmented by 1.15 kb in the targeted allele. Filters were hybridized with a fragment of mouse p47^{phox} cDNA (bp 18–1067) (24). Hybridization with exons 1 and 2 alone showed the same shift of the targeted band. Similar results were obtained with XbaI digested DNA. The neo^r probe hybridized only in the mutated allele. The upper band present in all lanes was a result of hybridization to exons 8 and distal. Wild type (+/+), heterozygote (+/−), and homozygote (−/−).
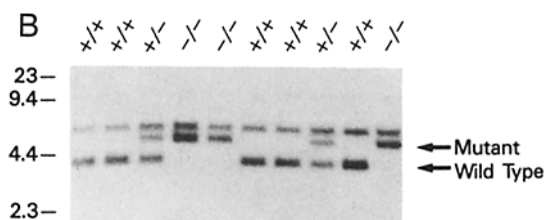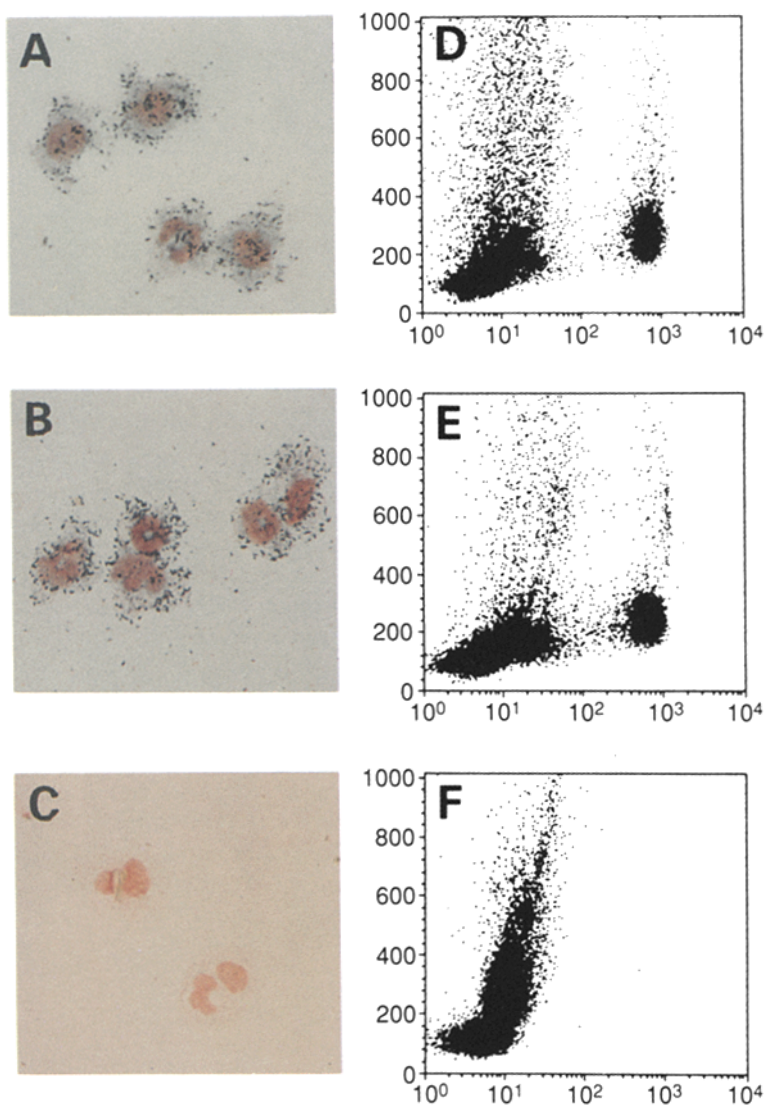
Figure 2. Respiratory burst impairment in p47$^{phox-/-}$ mice. PMA-stimulated NBT reduction was detected by blue-black granules in p47$^{phox+/+}$ (A) and p47$^{phox+/-}$ (B) phagocytes, whereas p47$^{phox-/-}$ (C) phagocytes did not reduce NBT. Two to six representative neutrophils are shown in each panel (×630). PMA-stimulated oxidation of dihydrorhodamine 123 to rhodamine 123 by whole blood was detected as fluorescent cells in the granulocyte gate. The y axis records side scatter and the x axis fluorescence intensity. p47$^{phox+/+}$ (D) and p47$^{phox+/-}$ (E) blood have similar populations of dihydrorhodamine-oxidizing neutrophils, whereas no p47$^{phox-/-}$ (F) phagocytes oxidize dihydrorhodamine. 25,000 live cell events were collected per sample and are represented as dots. Data are representative of six animals in each group.

heparin, and 25 μl was removed for total leukocyte and differential counts. HBSS and 2.5 × 10^6 log phase *S. aureus* were added to a final volume of 1 ml. The blood–bacteria suspension was rotated gently at 37°C for 20 min to allow phagocytosis of bacteria. Lysostaphin (Sigma) was added to a final concentration of 2.5 U/ml to eliminate extracellular bacteria, and the tubes were returned to 37°C (34). At 30 and 60 min after the addition of bacteria, 10-μl aliquots were lysed in distilled water and plated in soft agar. Colonies were enumerated at 24–48 h.

Intraperitoneal Thioglycollate Challenge. Mice (6–15 wk-old littermates) were injected intraperitoneally with 2 ml sterile thioglycollate (3% wt/vol) (35). Peritoneal exudates were collected after 5 h by peritoneal lavage with 10 ml PBS. The total leukocyte count and differential were determined by a hemocytometer.

Results

Generation of p47$^{phox-/-}$ Mice. We targeted exon 7 (amino acid 221) of the mouse p47^{phox} gene, a region known to be necessary for human p47^{phox} function (Fig. 1 *A* and reference 14). ES cells were transfected with the targeting vector and selected in the presence of G418 (28). Resistant colonies were screened for homologous recombination by PCR (27), and positive clones were confirmed by Southern hybridization. Electroporation of 3.5 × 10^7 total ES cells yielded 1,329 G418-resistant colonies, from which four homologous recombinant clones were confirmed. Blastocyst microinjection of two of these clones resulted in high level chimerism of three male offspring. Two of these males were fertile and showed germline transmission of the disrupted p47^{phox} gene (Fig. 1 *B*). Heterozygote matings yielded a distribution of wild-type (+/+)/heterozygote (+/−)/homozygote (−/−) progeny of 0.47:1.0:0.52, excluding embryonic lethality. Mice were genotyped by tail or ear biopsy at 3–4 wk of age, and tail venisection was performed aseptically at 4–6 wk of age without complications. Before the development of severe infections, p47$^{phox-/-}$ mice were fertile, of comparable weight to their unaffected littermates, and had normal peripheral blood total and differential leukocyte counts.

The p47$^{phox-/-}$ Phenotype. To determine that we had suc-

cessfully generated the biochemical phenotype of CGD, we tested phorbol myristate acetate stimulated phagocytes for evidence of superoxide production. As is true in human CGD patient phagocytes, p47$^{phox-/-}$ phagocytes did not reduce NBT to blue-black formazan (29–32), whereas p47$^{phox+/-}$ and p47$^{phox+/+}$ phagocytes reduced NBT normally (Fig. 2 A–C). This result was confirmed by a highly sensitive whole-blood assay that measures the conversion of nonfluorescent dihydrorhodamine 123 to fluorescent rhodamine 123 (Fig. 2 D–F and reference 33).

Defective Staphylococcal Killing In Vitro. Despite many functional similarities between mouse and human phagocytes, important differences have been noted, such as the absence of defensins from mouse phagocytes (36) and the lack of clear evidence of nitric oxide production by human phagocytes (37). Therefore, the possibility of compensatory NADPH oxidase–independent bactericidal pathways in the mouse was addressed by measuring the ability of whole blood to kill *Staphylococcus aureus* in vitro (34). Whole blood from p47$^{phox-/-}$ mice killed 10-fold fewer organisms than p47$^{phox+/-}$ or p47$^{phox+/+}$ mice after 30 or 60 min of incubation (P <0.001 and P <0.04, respectively; Fig. 3). The inclusion of lysostaphin, an enzyme that kills extracellular *S. aureus*, in this assay indicates that the differences in staphylococcal viability between the groups reflected differences in intracellular microbicidal activity. The numbers of Gram stain–identifiable organisms per phagocyte at 60 min were 0.8 ± 0.11 for p47$^{phox+/+}$ vs 1.67 ± 0.27 for p47$^{phox-/-}$ mice (P = 0.041).

Elimination of phagocyte NADPH oxidase activity in the mouse was therefore not completely compensated by some other staphylococcidal pathway.

Abnormally Exuberant Inflammation In Vivo. Aberrant inflammation in CGD may reflect infection, either cryptic or overt, or dysregulation of the inflammatory response. In humans with CGD, the inflammatory response in Rebuck skin windows is abnormally exuberant and prolonged (5). To determine whether p47$^{phox-/-}$ mice had a similar phenotype, we injected mice intraperitoneally with the sterile irritant thioglycollate (35). Peritoneal fluid total and differential leukocyte counts were done at 5 h after injection (Fig. 4). Twice as many total leukocytes were recruited into the peritoneal cavities of the p47$^{phox-/-}$ mice compared to their p47$^{phox+/-}$ and p47$^{phox+/+}$ littermates (P <0.001 and P = 0.001, respectively). The percentage of neutrophils was comparable in the three genotypes. Since this was found at an early time point, it likely represents a response to the stimulus and not a failure of cells to senesce or return to the circulation. This process may reflect a failure to degrade chemotactic signals, as has been previously hypothesized (5, 38). These signals may now be assayed directly and will be informative in the understanding of the aberrant inflammatory process in CGD.

Pathology of p47$^{phox-/-}$ Mice Mimics Human CGD. p47$^{phox-/-}$ mice spontaneously developed severe infections with types of organisms characteristic of human CGD, whereas no p47$^{phox+/+}$ or p47$^{phox+/-}$ mice maintained under the same conditions developed infections (P <0.001, Fig. 5). Gross, histopathologic, and microbiologic results of necropsies per-
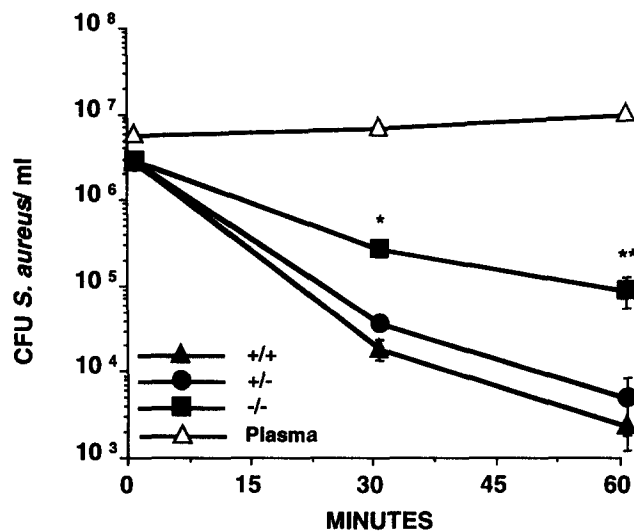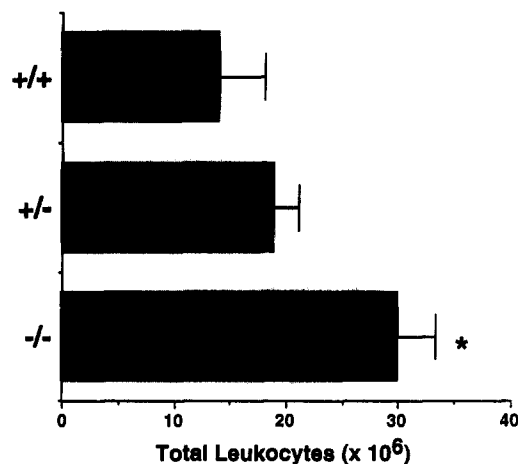

Figure 3. Impaired staphylococcal killing by whole blood in p47$^{phox-/-}$ mice. Log phase staphylococci were added to whole blood at time 0. Lysostaphin was added at 20 min of incubation and aliquots were removed at 30 and 60 min for enumeration of CFU of *S. aureus*. Assays were performed in duplicate on 5–11 wk-old littermates (n = 6 per group). Incubation of *S. aureus* in plasma alone was performed without lysostaphin. Data from two experiments are presented as means with SE. At 30 and 60 min, p47$^{phox-/-}$ whole blood permitted more staphylococci to survive than either p47$^{phox+/+}$ or p47$^{phox+/-}$ whole blood (P <0.02 and P <0.042, respectively). Comparisons were made by the unpaired Student's t test (Statworks, Philadelphia, PA).

Figure 4. Abnormally exuberant thioglycollate peritonitis in p47$^{phox-/-}$ mice. Thioglycollate was injected into the peritoneal cavities of 6–15-wk-old littermates, peritoneal exudates were collected 5 h later, and total peritoneal leukocyte number and differential counts were determined (n = 9 per group). The p47$^{phox-/-}$ mice had more peritoneal leukocytes after thioglycollate challenge compared to p47$^{phox+/+}$ or p47$^{phox+/-}$ mice (P = 0.001 and P <0.001, respectively). Differential counts on cytospin specimens were performed on six animals per group and showed no significant differences between the genotypes (78, 75, and 81% neutrophils, respectively). Data from three experiments are presented as mean with SE. Comparisons were made by the unpaired Student's t test (Statworks).
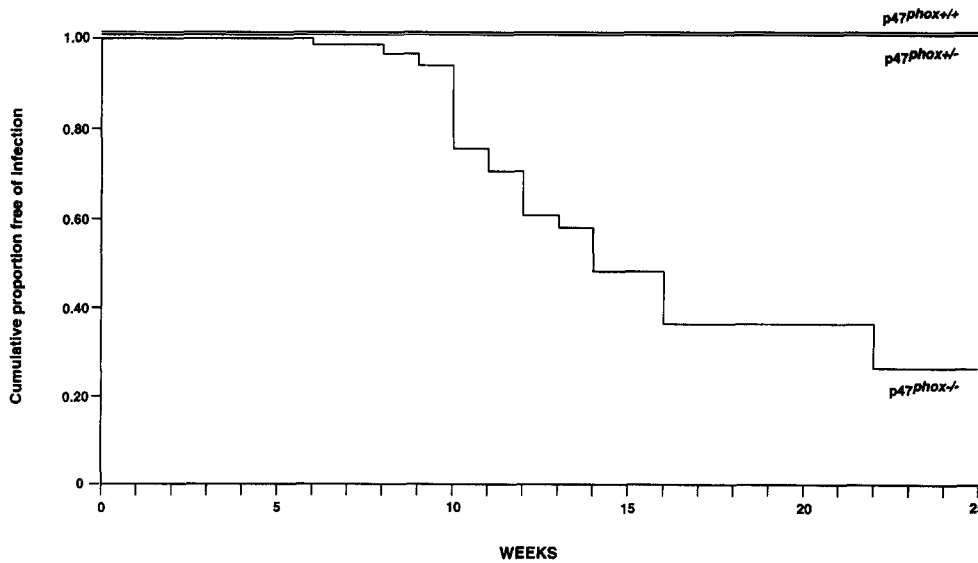
Figure 5. The Kaplan-Meier product probability of infection-free survival for 60 p47$^{phox-/-}$, 47 p47$^{phox+/-}$, and 28 p47$^{phox+/+}$ mice. p47$^{phox-/-}$ mice spontaneously developed severe infections confirmed at necropsy, whereas p47$^{phox+/-}$ and p47$^{phox+/+}$ animals did not (P <0.001). Differences between groups were determined by computation of the logrank statistic (42).

formed on six p47$^{phox-/-}$ mice from the initial cohort of animals are presented (Table 1). The deep infections were caused by *Staphylococcus xylosus* in two animals, a hyaline septate mold and *Lactobacillus* in one animal, and the fungus *Paecilomyces* in one animal. These organisms are similar (*S. xylosus*) or identical (*Paecilomyces*) to those that cause life-threatening infections in human CGD patients (1–4, 39). Four of the p47$^{phox-/-}$ animals had generalized adenopathy and splenomegaly. Gross and pathologic findings from one animal with disseminated *S. xylosus* are presented (Fig. 6). Histology showed granulomatous pneumonitis with neutrophils, plasma cells, lymphocytes, macrophages, and multinucleated giant cells. The initial cohort (eight p47$^{phox-/-}$ animals) was

identified by sterile metal ear tags aseptically placed, which may have caused local ear infection in the p47$^{phox-/-}$ animals. Subsequent observations in 52 p47$^{phox-/-}$ animals without ear tags, however, showed the same rates and types of infections. Therefore, as is seen in human CGD, absence of phagocyte NADPH oxidase activity in the mouse causes susceptibility to severe visceral infections.

Discussion

We have created a mouse with the same biochemical, functional, infection susceptibility, and pathological defects found in human CGD. The fidelity of this phenotype to human

Table 1. *Clinical, Microbiological, and Histopathological Characteristics of Necropsied p47$^{phox-/-}$ Mice*

Animal	Sex/age at necropsy	External lesions	Associated pathology	Abscesses	Granulomas	Microbiology
1	F/15 wk	Ear	Lymphadenopathy	Ear	–	S. xylosus
		Feet	Splenomegaly	Feet	–	S. xylosus
				Lung	+	S. xylosus
2	F/15 wk	Ear	Lymphadenopathy	Ear	–	S. xylosus
			Splenomegaly	Lung	+	S. xylosus
3	M/9 wk	None	None	Lung	+	Septate hyaline mold*
						Lactobacillus
4	F/11 wk	Ear	Lymphadenopathy	None	+	None
			Splenomegaly			
5	F/13 wk	Ear	Lymphadenopathy	Lung	+	Paecilomyces
			Splenomegaly			
6	F/8 wk	None	Lymphadenopathy	None	–	None

Animals listed were from the initial ear-tagged cohort. Animals without ear tags had similar pathology.
* Fungal elements seen on Gomori methenamine silver staining of lung tissue; fungal cultures were not performed.
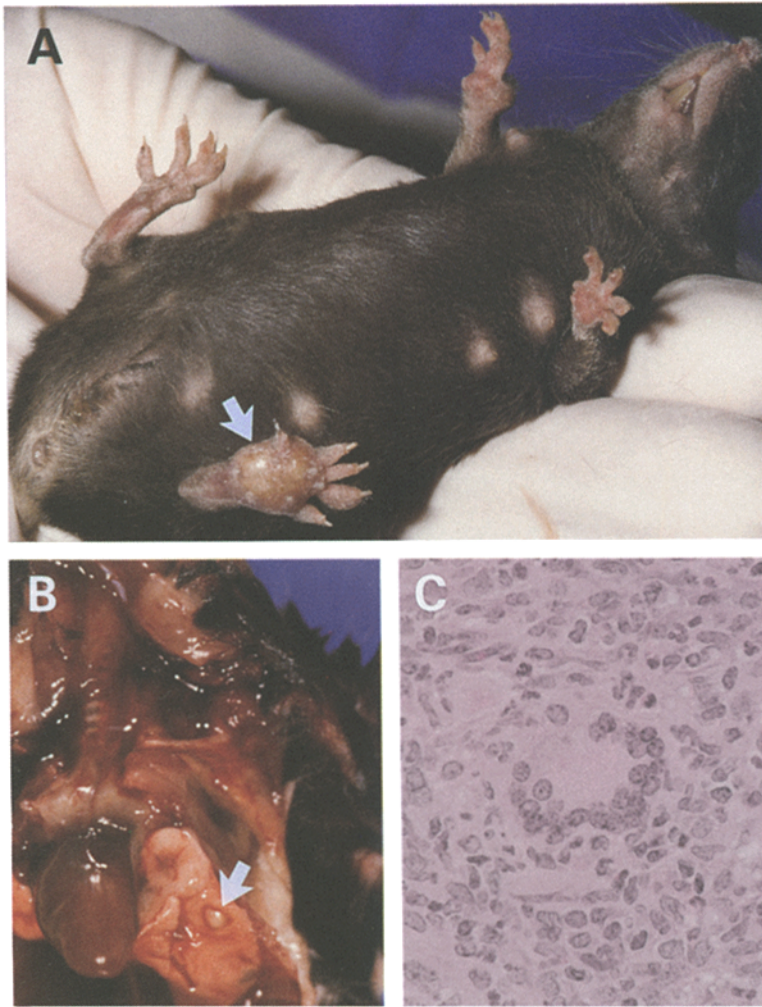
755   Jackson et al.

Figure 6. Gross and pathologic anatomy of disseminated *S. xylosus* infection in a p47*phox*−/− mouse. (*A*) An abscess of the left hindpaw (*arrow*) of a 15-wk-old female. This mouse also had cutaneous abscesses of the right periauricular soft tissue and the right forepaw. The lesions were fluctuant and grew *S. xylosus* in culture. (*B*) Necropsy of the mouse shown in *A*. A 5-mm pyogranuloma of the right caudal lobe of the lung is indicated (*arrow*). (*C*) Multinucleated giant cells were found throughout the inflammatory lung tissue indicated in *B*. Characteristic granulomatous inflammation was found interspersed with acute inflammation (hematoxylin and eosin stain, ×630).

CGD shows that there are no other biochemical systems in the mouse that completely compensate for the loss of products of the NADPH oxidase system. The p47*phox*−/− mouse is therefore likely to be informative for the exploration of NADPH oxidase mediated functions in infectious and inflammatory processes. The hypothesized roles for superoxide and related species in the pathogenesis of atherosclerosis, cataract formation, carcinogenesis, vasculitis, reperfusion injury, and aging can now be defined (8, 9).

Pollock et al. have created a homologous recombinant mouse model of the X-linked gp91*phox*-deficient form of CGD (40). Their animals showed no NBT or cytochrome C reduction, had abnormally exuberent thioglycollate responses, and were more susceptible to infections with the human pathogens *S. aureus* and *Aspergillus fumigatus*. However, these infections had to be induced in their animals and, once induced, did not cause granulomatous inflammation. Abnormally abundant intraperitoneal thioglycollate responses seen in the gp91*phox*−/− model were modest at 4 h after instillation but pronounced at later time points. The p47*phox*−/− animals also had abnormally abundant recruitment of neutrophils into the perito-

neal cavity after thioglycollate instillation, but at an earlier time point. In contrast to the X-linked gp91*phox*−/− model, the p47*phox*−/− animals developed high rates of spontaneous infection with a common mouse bacteria, *S. xylosus* (41), as well as the characteristic CGD infection *Paecilomyces* (39), confirming the critical role of the NADPH oxidase in protection of the mouse against rodent as well as human pathogens. Furthermore, unlike the X-linked gp91*phox*−/− model, the p47*phox*−/− animals developed granulomatous inflammation at sites of infection. The absence of granulomatous inflammation in the model of Pollock et al. may be caused by the relatively short duration of infection before death. The differences in infection susceptibility, histopathology, and inflammatory response may reflect intrinsic differences in our models of X-linked and autosomal recessive CGD, such as the absence of the cytochrome b_{558} complex in the gp91*phox*−/− model. These findings are somewhat at variance with the human disease, in which there is little phenotypic difference between the different genotypes of CGD. Since the p47*phox*−/− and gp91*phox*−/− animal models have been produced and bred into similar genetic backgrounds and maintained under similar

conditions, these differences may be significant. Comparison of these models under identical circumstances will be required to sort out these differences.

Our animal model of p47^{phox} deficiency mimics human

CGD and will permit definitive studies of the possible roles for the NADPH oxidase. Finally, this model will be informative for testing immune modulators and human gene therapeutics for CGD in vivo.

References

1. Gallin, J.I., and H.L. Malech. 1990. Update on chronic granulomatous diseases of childhood. *J. Am. Med. Assoc.* 263:1533–1537.
2. Gallin, J.I., E.S. Buescher, B.E. Seligmann, J. Nath, T. Gaither, and P. Katz. 1983. Recent advances in chronic granulomatous disease. *Ann. Intern. Med.* 99:657–674.
3. Muoy, R., A. Fischer, E. Vilmer, R. Seger, and C. Grisecelli. 1989. Incidence, severity and prevention of infections in chronic granulomatous disease. *J. Pediatr.* 114:555–560.
4. Forrest, C., J.R. Forehand, R.A. Axtell, R.L. Roberts, and R.B. Johnston. 1988. Clinical features and current management of chronic granulomatous disease. *Hematol. Oncol. Clin. N. Am.* 2:253–264.
5. Gallin, J.I., and E.S. Buescher. 1983. Abnormal regulation of inflammatory skin responses in male patients with chronic granulomatous disease. *Inflammation.* 7:227–232.
6. Ament, M., and H. Ochs. 1973. Gastrointestinal manifestations of chronic granulomatous disease. *N. Engl. J. Med.* 288:382–387.
7. Walther, M.M., H. Malech, A. Berman, P. Choyke, D.J. Venzon, W.M. Marston, and J.I. Gallin. 1992. The urological manifestations of chronic granulomatous disease. *J. Urol.* 147:1314–1318.
8. Johnson, K.J., and P.A. Ward. 1981. Role of oxygen metabolites in immune complex injury of lung. *J. Immunol.* 126:2365–2369.
9. Nathan, C.F., and Z.A. Cohn. 1981. Antitumor effects of hydrogen peroxide in vivo. *J. Exp. Med.* 154:1539–1553.
10. The International CGD Cooperative Study Group. 1991. A controlled trial of interferon gamma to prevent infection in chronic granulomatous disease. *N. Engl. J. Med.* 324:509–516.
11. Royer-Pokora, B., L.M. Kunkel, A.P. Monaco, S.C. Goff, P.E. Newburger, R.L. Baehner, F.S. Cole, J.T. Curnutte, and S.H. Orkin. 1986. Cloning the gene for an inherited human disorder-chronic granulomatous disease- on the basis of its chromosomal location. *Nature (Lond.).* 322:32–38.
12. Parkos, C.A., M.C. Dinauer, A.J. Jesaitis, S.H. Orkin, and J.T. Curnutte. 1988. Primary structure and unique expression of the 22-kilodalton light chain of human neutrophil cytochrome b. *Proc. Natl. Acad. Sci. USA.* 85:3319–3323.
13. Lomax, K.J., T.L. Leto, H. Nunoi, J.I. Gallin, and H.L.

Malech. 1989. Recombinant 47-kilodalton cytosol factor restores NADPH oxidase in chronic granulomatous disease. (published correction appears in *Science.* Vol. 246, 1990, p. 987.) *Science (Wash. DC).* 245:409–412.
14. Volpp, B.D., W.M. Nauseef, J.E. Donelson, D.R. Moser, and R.A. Clark. 1989. Cloning of the cDNA and functional expression of the 47-kilodalton cytosolic component of human neutrophil respiratory burst oxidase. (published correction appears in *Proc. Natl. Acad. Sci. USA.*, Vol. 86, 1989, p. 9563.) *Proc. Nat. Acad. Sci. USA.* 86:7195–7197.
15. Leto, T.L., K.J. Lomax, B.D. Volpp, H. Nunoi, J.M. Sechler, W.M. Nauseef, R.A. Clark, J.I. Gallin, and H.L. Malech. 1990. Cloning of a 67-kD neutrophil oxidase factor with similarity to a noncatalytic region of p60^{c-src}. *Science (Wash. DC).* 248:727–730.
16. Abo, A., E. Pick, A. Hall, N. Totty, C.G. Teahan, and A.W. Segal. 1991. Activation of the NADPH oxidase involves the small GTP-binding protein p21^{rac1}. *Nature (Lond.).* 353:668–670.
17. Leto, T.L., A.G. Adams, and I. DeMendez. 1994. Assembly of the phagocyte NADPH oxidase: binding of Src homology domains to proline-rich targets. *Proc. Natl. Acad. Sci. USA.* 91:10650–10654.
18. Clark, R.A., H.L. Malech, J.I. Gallin, H. Nunoi, B.D. Volpp, D.W. Pearson, W.M. Nauseef, and J.T. Curnutte. 1989. Genetic variants of chronic granulomatous disease: prevalence of deficiencies of two cytosolic components of the NADPH oxidase system. *N. Engl. J. Med.* 321:647–652.
19. Casimir, C.M., H. Bu-Ghanim, A.R. Rodaway, D.L. Bentley, P. Rowe, and A.W. Segal. 1991. Autosomal recessive chronic granulomatous disease caused by deletion at a dinucleotide repeat. *Proc. Natl. Acad. Sci. USA.* 88:2753–2757.
20. Dinauer, M.C., E.A. Pierce, G.A.P. Bruns, J.T. Curnutte, and S.H. Orkin. 1990. Human neutrophil cytochrome b light chain (p22-phox). Gene structure, chromosomal location, and mutations in cytochrome-negative autosomal recessive chronic granulomatous disease. *J. Clin. Invest.* 86:1729–1737.
21. Roos, D. 1994. The genetic basis of chronic granulomatous disease. *Immunol. Rev.* 138:121–157.
22. Xie, Q.-W., H.J. Cho, J. Calaycay, R.A. Mumford, K.M. Swiderek, T.D. Lee, A. Ding, T. Troso, and C.F. Nathan. 1992.

Cloning and characterization of inducible nitric oxide synthase from mouse macrophages. *Science (Wash. DC).* 256:225–228.

23. Ding, A.H., C.F. Nathan, and D.J. Stuehr. 1988. Release of reactive nitrogen intermediates and reactive oxygen intermediates from mouse peritoneal macrophages. *J. Immunol.* 141:2407–2412.

24. Jackson, S.H., H.L. Malech, C.A. Kozak, K.J. Lomax, J.I. Gallin, and S.M. Holland. 1994. Cloning and functional expression of the mouse homologue of p47phox. *Immunogenetics.* 39:272–275.

25. Capecchi, M. 1989. Altering the genome by homologous recombination. *Science (Wash. DC).* 244:1288–1292.

26. Doetschman, T.C., H. Eistetter, M. Katz, W. Schmidt, and R. Kemler. 1985. The in vitro development of blastocyst-derived embryonic stem cell lines: formation of visceral yolk sac blood islands and myocardium. *J. Embryol. Exp. Morphol.* 87:27–45.

27. Ramirez-Solis, R., J. Rivera-Perez, J.D. Wallace, M. Wims, H. Zheng, and A. Bradley. 1992. Genomic DNA microextraction: a method to screen numerous samples. *Anal. Biochem.* 201:331–335.

28. Robertson, E.J. 1987. Teratocarcinomas and Embryonic Stem Cells: A Practical Approach. IRL Press, Oxford, England. pp. 71–75.

29. Metcalf, J.A., J.I. Gallin, W.M. Nauseef, and R.K. Root. 1986. Laboratory Manual of Neutrophil Function. Raven Press, New York. p. 100.

30. Gifford, R.H., and S.E. Malawista. 1970. A simple rapid micromethod for detecting chronic granulomatous disease of childhood. *J. Lab. Clin. Med.* 75:511–519.

31. Baehner, R.L., and D.G. Nathan. 1968. Quantitative nitroblue tetrazolium test in chronic granulomatous disease. *N. Engl. J. Med.* 278:971–976.

32. Ochs, H.D., and R.P. Igo. 1973. The NBT slide test: a simple screening method for detecting chronic granulomatous disease and female carriers. *J. Pediatr.* 83:77–82.

33. Vowells, S.J., S. Sekhsaria, H.L. Malech, M. Shalit, and T.A. Fleisher. 1995. Flow cytometric analysis of the granulocyte respiratory burst: a comparison study of fluorescent probes. *J. Immunol. Methods.* 178:89–97.

34. Gallin, J.I., J.S. Bujak, E. Patten, and S.M. Wolff. 1974. Granulocyte function in the Chediak-Higashi syndrome of mice. *Blood.* 43:201–206.

35. Baron, E.J., and R.A. Proctor. 1982. Elicitation of peritoneal polymorphonuclear neutrophils from mice. *J. Immunol. Methods.* 49:305–313.

36. Eisenhauer, P.B., and R.I. Lehrer. 1992. Mouse neutrophils lack defensins. *Infect. Immun.* 60:3446–3447.

37. Murray, H.W., and R.F. Teitelbaum. 1992. L-arginine-dependent reactive nitrogen intermediates and the antimicrobial effect of activated human mononuclear phagocytes. *J. Infect. Dis.* 165:513–517.

38. Henderson, W.R., and S.J. Klebanoff. 1983. Leukotriene production and inactivation by normal, chronic granulomatous disease and myeloperoxidase deficient neutrophils. *J. Biol. Chem.* 258:13522–13527.

39. Williamson, P.R., K.J. Kwon-Chung, and J.I. Gallin. 1992. Successful treatment of *Paecilomyces varioti* infection in a patient with chronic granulomatous disease and a review of *Paecilomyces* species infections. *Clin. Infect. Dis.* 5:1023–1026.

40. Pollock, J.D., D.A. Williams, M.A.C. Gifford, L.L. Li, X. Du, J. Fisherman, S.H. Orkin, C.M. Doerschuk, and M.C. Dinauer. 1995. Mouse model of X-linked chronic granulomatous disease, an inherited defect in phagocyte superoxide production. *Nature Genet.* 9:202–209.

41. Brandfield, J.F., J.E. Wagner, G.P. Boivin, E.K. Steffen, and R.J. Russell. 1993. Epizootic fetal dermatitis in athymic nude mice due to *Staphylococcus xylosus*. *Lab. Animal Sci.* 43:111–113.

42. Dawson-Saunders, B., and R.G. Trapp. 1990. Basic and Clinical Biostatistics, Appleton & Lange, East Norwalk, CT. p. 199.